J. Biochem. **131**, 213–218 (2002)

Contribution of an Imidazole-Indole Stack to High Catalytic Potency of a Lysine-Specific Serine Protease, *Achromobacter* Protease I

Kentaro Shiraki,[1] Shigemi Norioka, Shaoliang Li, and Fumio Sakiyama[2]

The Institute for Protein Research, Osaka University, 2-1 Yamadaoka, Suita, Osaka 565-0871

Received November 2, 2001; accepted November 26, 2001

***Achromobacter* protease I (API), a lysine-specific serine-protease of the trypsin family, has an aromatic-ring stacking Trp 169–His 210 in close proximity to the reactive site. In order to investigate the role of this novel aromatic stacking, several mutants of the two residues were constructed and their kinetic parameters were determined. Three His 210 mutants showed lower activity by one order of magnitude than the wild-type with a peptide substrate of Ala-Ala-Lys-MCA (4-methylcoumaryl-7-amide), but 30–170% activity towards Val-Leu-Lys-MCA, suggesting that His 210 plays a role in keeping high activity toward various substrates by maintaining the active form of the substrate-binding subsite. Kinetic results of eight Trp 169 variants showed a roughly linear relation between k_{cat} or K_m values and the surface area at residue 169. With increasing size of the side-chain, k_{cat} values increased, while K_m values decreased. A systematic kinetic analysis of the activities of Trp 169 mutants toward Lys-MCA, Ala-Lys-MCA, and Ala-Ala-Lys-MCA peptide substrates revealed that large side-chain, rather than aromaticity, plays an important role in retaining the high catalytic activity of API. Due to the presence of the aromatic stacking, API shows one order of magnitude higher activity than bovine trypsin.**

Key words: aromatic stacking, catalytic triad, serine protease, site-directed mutagenesis.

Serine proteases play important physiological roles in various biological processes such as development, signal transduction, RNA translation, blood coagulation, immunity, and apoptosis (*1–6*). They are enzymes whose structures, functions, and mechanisms of catalysis are well understood (*7–10*). *Achromobacter* protease I (API, EC 3.4.21.50) is a trypsin-type serine protease secreted extracellularly by *Achromobacter lyticus* M497-1 (*11*). Amino acid sequence identity between API and bovine trypsin is as low as 20% (*12*). API is distinct from the trypsin type serine protease in its restricted lysine specificity, an order of magnitude higher peptidase activity, a broad pH optimum ranging from pH 8.5–10.5 and stability against denaturation with urea and SDS (*13, 14*). Due to these favorable properties as a protein-degrading enzyme, API is now a uniquely useful lysyl-endopeptidase for protein fragmentation (*15, 16*) and lysyl bond formation (*17*).

We have studied the structure-function relationship of API by X-ray crystallography and protein engineering in order to reveal the structural basis of the superior features of API. So far, the mechanism of lysine specificity has been shown to involve Asp 225, which is at the shallow S1-pocket in the active site (*18*). The three-dimensional structures of native and TLCK-inactivated API have been solved by X-ray crystallography at 1.2 and 2.0 Å resolution, respectively (protein data bank code of 1arb.pdb and 1arc.pdb). The apparent three-dimensional structure of API is quite similar to that of bovine trypsin. In the TLCK-modified enzyme, the active-site region is exclusively perturbed by the introduction of TLCK, which is covalently bound to His 57 in the catalytic triad composed by this 57 Asp 113 and Ser 194. Subsite mapping has revealed the presence of at least three subsites which extend to the N-terminal side of the scissile bond in the substrate, and His 210, Gly 211 and Gly 212 have been proposed as substrate-binding subsites S1, S2, and S3, respectively. API has His 210 at subsite S1, while other serine proteases have Ser (Fig. 1). In addition, crystallographic analysis revealed that the imidazole ring of His 210 is stacked with the indole ring of Trp 169, which is not directly involved in the constitution of the active site (Fig. 1). The novel aromatic interaction in the active site region may have a certain connection with the high catalytic potency of API, while API shows higher activity by one order of magnitude than bovine trypsin. The present paper deals with the analysis of kinetic parameters for several API mutants at both aromatic residues.

MATERIALS AND METHODS

Materials—Enzymes and peptide substrates were purchased from following sources: all restriction and modification enzymes from Takara (Kyoto), API from Wako Pure Chemical Industries (Osaka) and Boc-Val-Leu-Lys-MCA

[1] To whom correspondence should be addressed: School of Materials Science, Japan Advanced Institute of Science and Technology, 1-1 Asahidai, Tatsunokuchi, Ishikawa 923-1292. Tel: +81-761-51-1657, Fax: +81-761-51-1655, E-mail: kshiraki@jaist.ac.jp

[2] Present address: International Buddhist University, 3-2-1 Gakuen-mae, Habikino, Osaka 583-8501.

Abbreviations: API, *Achromobacter* protease I; Boc, *t*-butoxycarbonyl; MCA, CD, circular dichroism; 4-methylcoumaryl-7-amide; TLCK, *N*α-tosyl-L-lysyl chloromethyl ketone; UV, ultraviolet.

from the Peptide Institute (Osaka). Ovomucoid from hen egg white was from Sigma Chemical (St. Louis, Missouri). Boc-Val-Leu-Lys-MCA was from the Peptide Institute Inc. Boc-Lys-MCA, Boc-Ala-Lys-MCA, and Boc-Ala-Lys-MCA were prepared in our laboratory. All other chemicals were obtained from commercial suppliers and of the highest analytical grade.

Preparation and Purification of API Mutants—Single-stranded DNA for mutagenesis was obtained from plasmid pKYN200 (*19*). The mutagenesis was performed according to the Uracil-DNA mediated method (*20*). The mutagenic primers were: 5′-CGGCGCCGCCGCCXYZGGCCACGAACG-3′ for Trp 169 mutants [XYZ = GTA (Tyr), GAA (Phe), CAA (Leu), GTG (His), TAC (Val), TGC (Ala), and CCC (Gly)] and 5′-CGACGGGCCCCCXYZCAGCTGGCCGAGCAC-3′ for His 210 mutants [XYZ = GGC (Ala), GGA (Ser), and GAA (Phe)] where XYZ represents the mismatched bases for substituting sites. *Escherichia coli* strain JM109 was used for the preparation of plasmid and phage DNA. The mutant genes were identified by DNA sequencing and then subcloned into the expression vector pKYN200 (*19*). Transformants of *E. coli* strain JA221 cells were grown on Luria-Bertani medium supplemented with 50 μg/ml ampicillin. The expression and purification of each wild-type or mutant API was done as described previously (*16*). The amount of the mutant protein obtained from 2 liters of culture medium was 0.5–0.8 mg.

Determination of Kinetic Parameters—Lysylendopeptidase activity of each enzyme was measured with Boc-Lys-MCA, Boc-Ala-Lys-MCA, Boc-Ala-Ala-Lys-MCA, and Boc-Val-Leu-Lys-MCA as a substrate. Quantitative assay techniques were previously reported by our laboratory for API mutants using these substrates (*16*). Briefly, the substrate in 0.2 M Tris-HCl (pH 9.0) containing DMF (1%) was diluted with 0.2 M Tris-HCl (pH 9.0) to the desired final substrate concentration. After incubation for 10 min at 37°C, a portion (2 ml) of the substrate solution was mixed with 100 μl of a 2 nM enzyme solution. Increased fluorescence of liberated 7-amino-4-methylcoumarin was determined at 440 nm upon excitation at 380 nm with a Hitachi fluorescence spectrometer (F-4000). Each enzyme concentration was determined by amino acid composition analysis with a Hitachi L-8500S automatic amino acid analyzer. Values for the catalytic rate constant (k_{cat}) and the Michaelis constant (K_m) were obtained from initial velocity on theoretical curves calculated by nonlinear regression analysis and are shown as the average of at least three experiments.

Calculation of Accessible Surface Area of Individual Residues in API—The accessible surface area of individual residues in API was calculated with software of Daikin Comtec MOL-CLYS. Information on individual atoms of API was obtained from Protein Data Bank, code name: 1arb.pdb. For this calculation, the atoms of crystallized water molecules were removed from the data. The radius of the solvent probe was 1.4 Å.

RESULTS

Mutation, Expression, and Characterization of API Mutants—In the present investigation, His 210 and Trp 169 were selected as target amino acids for modification and separately mutated (Fig. 1). Three amino acids, Ala, Ser, and Phe, were chosen as substitutes for His 210. Substitution of the two aliphatic residues was designed to unravel the functional role of the imidazole ring, which may interact electrostatically with Asp 113. Phe was the sole aromatic substituent for testing whether aromaticity is sufficient for residue 210 to contribute to the enhancement of the catalytic potency of API. Seven amino acids, Tyr, Phe, His, Leu, Val, Ala, and Gly, were substituted for Trp 169. Mutation of Trp 169 was designed to examine whether aromaticity, hydrophobicity, size of the side chain at position 169, or a combination of these factors is necessary to generate and maintain the high catalytic potency of the lysylendopeptidase.

The DNA fragment of each mutant was chemically synthesized and integrated into an API expression vector. The mutation site in the cloned gene was confirmed by DNA sequencing. The mature mutated protein secreted into the periplasm in *E. coli* cells was purified and the molecular mass was confirmed for most purified proteins. Far UV-CD spectra revealed that all mutated enzymes retained the same backbone structure as native API (data not shown).

Kinetic Parameters for His 210 Mutants—The lysylen-

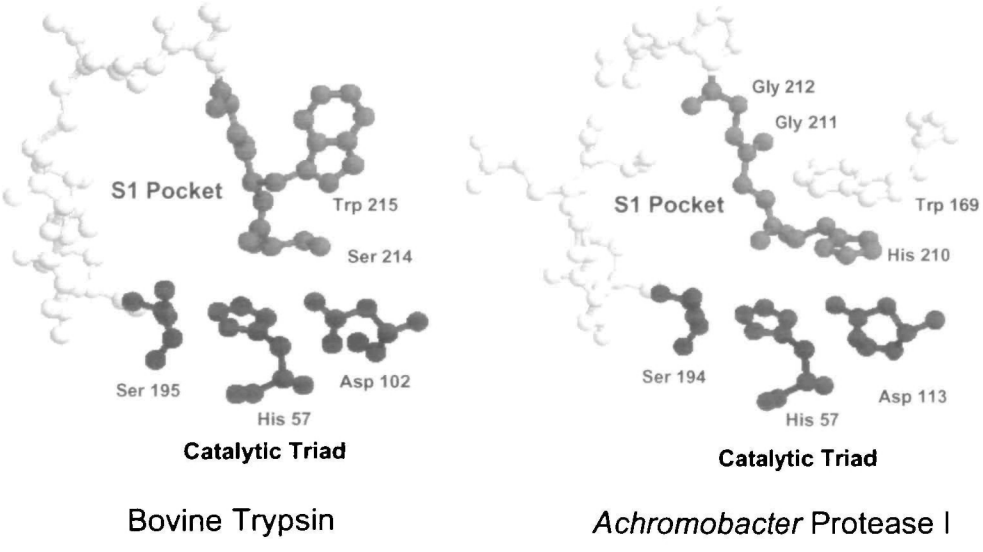

Fig. 1. **Ball-and-stick model of the active sites for *Achromobacter* protease I (API) and bovine trypsin.** Catalytic triad residues in API are Asp 113, His 57, and Ser 194. Catalytic triad residues in trypsin are Asp 102, His 57, and Ser 195. S1 pocket binds a lysyl side-chain of the substrate. Substrate-binding subsites in API and trypsin are His 210–Gly 211–Gly 212 and Ser 214–Trp 215–Gly 216, which are regions for stabilizing substrate-enzyme complex by several hydrogen bonds. API has a unique, protein-surface Trp 169 in proximity to the reactive site.

dopeptidase activity of three His 210 mutants, H210F, H210S, and H210A, was assayed with two synthetic tripeptide substrates, Boc-Ala-Ala-Lys-MCA and Boc-Val-Leu-Lys-MCA (Table I). With Boc-Ala-Ala-Lys-MCA, H210A and H210S were 12–14-fold less active than native API. A similar inactivation also took place with H210F, showing that the presence of an aromatic ring is not sufficient to maintain a high lysylendopeptidase activity. The lowering of k_{cat}/K_m for the three mutants was caused by a combination of decreased k_{cat} and increased K_m. With a more hydrophobic substrate, Boc-Val-Leu-Lys-MCA, every mutant behaved differently: the peptidase activity of H210A was slightly lost, whereas H210S was considerably activated (170% activity compared with native API). H210F was the least active of the three mutants. The increased activity of H210S was due to a 3-fold decrease of K_m. The decreased activity of H210F was due mainly to a 3-fold increase of K_m. The ratio of K_m estimated with Boc-Val-Leu-Lys-MCA to that estimated with Boc-Ala-Ala-Lys-MCA for native API, H210A, H210S, and H210F, was 0.75, 0.21, 0.12, and 0.73, respectively. These results suggests that the aromatic ring at the side chain of residue 210 serves to moderately lower K_m for a substrate that has hydrophobic subsites P2 and P3. Basically the k_{cat} tended to increase either with a hydrophobic substrate or in the presence of an aromatic ring at residue 210. In fact, the ratio of k_{cat} estimated with Boc-Val-Leu-Lys-MCA to that estimated with Boc-Ala-Ala-Lys-MCA for native API, H210A, H210S, and H210F was 0.95, 3.0, 2.8, and 1.8, respectively, which showed that non-aromatic 210 mutants much favored the hydrophobic substrate. These results indicate that His 210 generates the high catalytic potency of API by decreasing K_m and by increasing k_{cat}.

Kinetic Parameters for Trp 169 Mutants.—(i) Kinetics with Boc-Val-Leu-Lys-MCA: Kinetic parameters of seven Trp 169 mutants, W169Y, W169F, W169H, W169L, W169V, W169A, and W169G, were determined using Boc-Val-Leu-Lys-MCA as a substrate (Table II). All mutants assayed were less active than native API. Tyr, Phe, and Leu mutants retained 25–45% endopeptidase activities. These results imply that hydrophobicity rather than aromaticity at residue 169 is important to express high catalytic activity of API. However, W169H was only 10% active, which was due mainly to an 8-fold increase in its K_m. This indicates that hydrophobicity rather than aromaticity at residue 169 contributes to an increase in k_{cat}/K_m. W169A and W169G, which have neither a hydrophobic nor an aromatic ring at position 169, were >200-fold less active relative than the native enzyme. To decide whether hydrophobicity or size of the side chain at residue 169 is primarily responsible for high catalytic potency, kinetic parameters were plotted as a function of surface area, which represents the size of the side chain in free amino acid (Fig. 2). With increasing size of the side-chain at residue 169, k_{cat} values increased, while K_m values decreased. The k_{cat} *versus* surface area relation was roughly linear, while K_m *versus* surface area relation showed less linearity due to the deviation of the W169H value.

(ii) Kinetics with Boc-(Ala)$_{0-2}$-Lys-MCA: To investigate the effect of subsite interaction on the peptidase activity, kinetic parameters were determined for six Trp 169 mutants using Boc-(Ala)$_{0-2}$-Lys-MCA (Table III). Several interesting features were found in this experiment. First, the lysylendopeptidase activity of all mutants increased as the sub-

TABLE I. **Kinetic constants of three His210 mutants as obtained with Boc-Ala-Ala-Lys-MCA and Boc-Val-Leu-Lys-MCA as substrate at pH 9.0 and 37°C.**

Enzyme	Substrate	K_m (μM)	k_{cat} (s^{-1})	k_{cat}/K_m (μM^{-1} s^{-1})
Wild-type	AAK	2.8 ± 0.2	98 ± 12	35 ± 7
	VLK	2.1 ± 0.2	93 ± 10	44 ± 9
H210S	AAK	6.0 ± 0.3	18 ± 4	3.0 ± 0.7
	VLK	0.7 ± 0.1	52 ± 5	74 ± 18
H210A	AAK	6.1 ± 0.3	15 ± 3	2.5 ± 0.6
	VLK	1.3 ± 0.2	45 ± 5	35 ± 9
H210F	AAK	10.0 ± 0.3	51 ± 6	5.0 ± 0.7
	VLK	7.3 ± 0.3	96 ± 14	13 ± 3

TABLE II. **Kinetic constants of seven Trp169 mutants as obtained with Boc-Val-Leu-Lys-MCA as substrate at pH 9.0 and 37°C.**

Enzyme	K_m (μM)	k_{cat} (s^{-1})	k_{cat}/K_m (μM^{-1} s^{-1})
Wild-type	2.1 ± 0.2	93 ± 10	44 ± 9
W169Y	4.3 ± 0.1	83 ± 9	19 ± 3
W169F	3.6 ± 0.3	71 ± 12	20 ± 5
W169L	3.4 ± 0.3	36 ± 8	11 ± 3
W169H	17 ± 0.4	67 ± 15	4.0 ± 0.7
W169V	10 ± 1	28 ± 9	2.8 ± 1.1
W169A	20 ± 1	4.6 ± 1.2	0.23 ± 0.07
W169G	32 ± 1	0.8 ± 0.2	0.030 ± 0.003

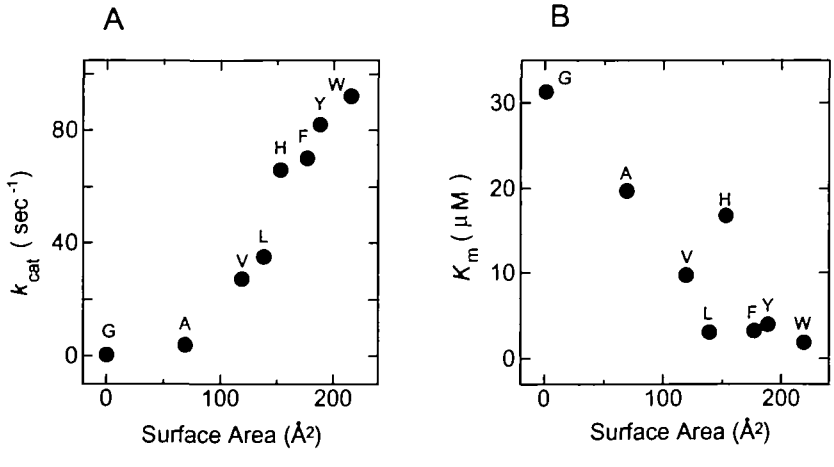

Fig. 2. **Relationship between k_{cat} (A) and K_m (B) and surface area of amino acids at position 169 in seven Trp 169 mutants.** Boc-Val-Leu-Lys-MCA was used as substrate, and the surface areas of amino acids are from the literature (*23*). G, A, V, L, H, F, Y, and W denote Gly, Ala, Val, Leu, His, Phe, Tyr, and Trp, respectively.

strate peptide chain length increased, and the presence of at least three subsites (S1, S2, and S3) was confirmed. Second, the peptidase activity of API decreased to 1/320 upon loss of the indole ring at residue 169 (W169A), even though all three subsites may be involved in the binding of substrate. In this case, a 38-fold reduction of k_{cat} was a major cause of the inactivation. Third, W169L was 8.5-fold more active than W169H, of which the lower enzyme activity was due to a 5.2-fold increase of K_m relative to the Leu mutant. These data indicate that catalytic activity is enhanced by the contribution of hydrophobicity rather than aromaticity at residue 169. On the other hand, the relationship between K_m and substrate chain length unraveled the contribution of the side chain of residue 169 to the potentiation of substrate binding with subsite (Table III). It is obvious that Trp 169 strengthens the binding of substrate at subsites S1-S2 and S1-S2-S3 to the same extent. This binding potential was reduced by changing the indole side chain to a smaller and less hydrophobic one.

(iii) Size and hydrophobicity of the side chain of residue 169: To explore factors which enhance lysylendopeptidase activity, the k_{cat} and K_m values relative to those of native API were calculated for the six Trp 169 mutants based on kinetic data (Table III) and plotted as a function of size of the side chain at residue 169 (Fig. 3). Although some plots deviated from linearity, the k_{cat}-surface area relation was essentially linear irrespective of the peptide chain length of substrate, suggesting that the size and hydrophobicity of the side chain is primarily responsible for the high enzyme activity. The plotting of K_m against surface area clearly showed that the binding of Boc-Lys-MCA at subsite S1 has no relation with the size and hydrophobicity at the side chain of residue 169.

TABLE III. **Kinetic constants of six Trp169 mutants as obtained with Boc-(Ala)$_{0-2}$-Lys-MCA as substrate at pH 9.0 and 37°C.**

Enzyme	Substrate	K_m (μM)	k_{cat} (s^{-1})	k_{cat}/K_m ($\mu M^{-1}\ s^{-1}$)
Wild-type	K	38 ± 1	8.4 ± 3.1	0.22 ± 0.08
	AK	3.7 ± 0.3 (10%)	46 ± 8	12 ± 4
	AAK	2.8 ± 0.2 (7%)	98 ± 10	35 ± 7
W169Y	K	37 ± 1	5.2 ± 2.2	0.14 ± 0.06
	AK	7.2 ± 0.6 (19%)	22 ± 11	3.1 ± 1.9
	AAK	6.3 ± 0.4 (17%)	40 ± 7	6.3 ± 1.9
W169F	K	29 ± 1	6.0 ± 1.1	0.21 ± 0.04
	AK	5.8 ± 0.3 (20%)	24 ± 4	4.1 ± 1.0
	AAK	4.0 ± 0.5 (14%)	48 ± 9	12 ± 4
W169L	K	46 ± 2	4.5 ± 1.4	0.10 ± 0.03
	AK	9.9 ± 0.3 (22%)	31 ± 4	3.2 ± 0.4
	AAK	4.6 ± 0.4 (10%)	37 ± 6	8.0 ± 2.2
W169H	K	74 ± 3.8	2.7 ± 0.9	0.04 ± 0.01
	AK	34 ± 1 (46%)	11 ± 3	0.31 ± 0.08
	AAK	24 ± 1 (32%)	23 ± 3	0.94 ± 0.20
W169V	K	81 ± 2.2	2.3 ± 0.7	0.03 ± 0.01
	AK	42 ± 1 (52%)	7.0 ± 0.6	0.17 ± 0.02
	AAK	12 ± 1 (15%)	20 ± 6	1.7 ± 0.6
W169A	K	66 ± 2.1	0.4 ± 0.2	0.006 ± 0.003
	AK	34 ± 2 (52%)	1.1 ± 0.4	0.032 ± 0.015
	AAK	23 ± 2 (35%)	2.6 ± 0.8	0.11 ± 0.05

Substrates K, AK, and AAK are Boc-Lys-MCA, Boc-Ala-Ala-Lys-MCA, and Boc-Ala-Ala-Lys-MCA, respectively. Parentheses in K_m show the relative K_m values of Boc-Ala-Ala-Lys-MCA and Boc-Ala-Ala-Lys-MCA defined by K_m value of Boc-Lys-MCA as 100%.

DISCUSSION

Since H210S was shown to be a more active enzyme than native API, the imidazole ring of His 210 is not indispensable for high lysylendopeptidase activity in the hydrolysis of Boc-Val-Leu-Lys-MCA. This is reminiscent of structural characteristics inherent in the chymotrypsin family, in which Ser/Thr is usually found at subsite S1. However, with less hydrophobic Boc-Ala-Ala-Lys-MCA, His 210 played a pivotal role in both the enhanced affinity for substrate and the acceleration of the hydrolysis of lysyl bond. The contribution of the hydrophobic environment around subsites S1 and S2 to efficient substrate binding and the subsequent catalytic process was indicated. This hydrophobic effect was significant in the case of H210S. It can be noted that the presence of His 210 at subsite S1 is critical in the generation of high k_{cat}/K_m values for both hydrophobic and hydrophilic lysine substrates. As is seen for W169F, the imidazole ring at residue 210 is essentially replaceable by a benzene ring, even though the K_m is greater than that of native API. This is probably due to local structural disorder caused by imperfect packing of the benzene ring in place of the His 210 imidazole ring that makes contact with the His 177 imidazole ring (2.7 Å for His 210 Nδ1-His 177 Nε2). It is thus suggested that the aromatic-aromatic inter-

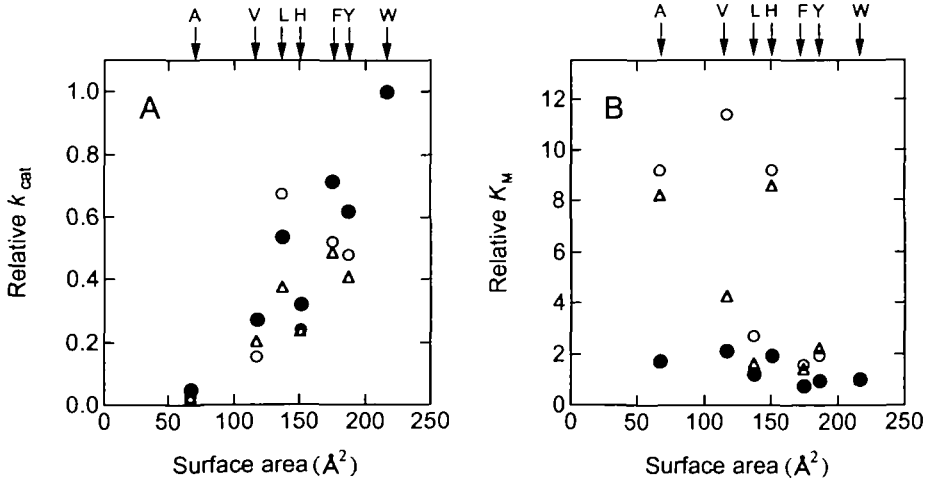

Fig. 3. **Relationship between relative k_{cat} (A) and K_m (B) and surface area of amino acids at position 169 of six Trp 169 mutants.** Relative k_{cat} and K_m values of mutant enzymes were defined by those of wild-type API as 1.0. Kinetic parameters were determined with Boc-Lys-MCA (closed circles), Boc-Ala-Lys-MCA (open circles), and Boc-Ala-Ala-Lys-MCA (open triangle). G, A, V, L, H, F, Y, and W denote Gly, Ala, Val, Leu, His, Phe, Tyr, and Trp, respectively.

action between His 210 and Trp 169 builds up a stable, local conformation around subsite S1, and thereby API efficiently hydrolyzes a wide range of substrates at the lysyl bond. Of course, this is only one of the roles that His 210 plays, and the possibility of other roles in the generation and/or control of high catalytic potency of API is not ruled out.

In addition to His 210, Trp was found to be the best amino acid at position 169. The side chain of this aromatic amino acid is the largest and most hydrophobic among protein amino acids, making it possible for API to attain the efficient substrate binding and substrate turnover during catalysis. In the present investigation, it was shown that k_{cat} was affected by the size and hydrophobicity of the side chain of residue 169 only in the presence of the S2-P2 and S3-P3 interactions: k_{cat} increases linearly as the side chain increases its size and hydrophobicity. In native API, the scissile lysyl bond must be properly oriented to a defined position to enable the nucleophilic attack by the Ser 194 hydroxyl in the enzyme-substrate complex. Such favorable orientation of the substrate toward the catalytic site is likely to be ensured by the His 210-Trp 169 pair for dipeptide and longer peptide substrates. Trp 169 has actually little effect on the k_{cat} with an acyl lysine substrate lacking subsites P2 and P3. A similar subsite potentiation effect by an adjacent aromatic residue is absent in bovine trypsin though Trp 215 exists at subsite S2 (*21*).

Correlation of K_m with the size of the side chain of residue 169 was not simple (Fig. 3). As in the case of k_{cat}, the S1–P1 interaction was not affected by the nature of residue 169, as expected from its distant location to subsite S1. The S2–P2 interaction was so strong that the S3–P3 interaction became trivial in native API (Table III). W169Y and W169F retained the same tendency, suggesting that the presence of an aromatic residue at position 169 strengthens substrate binding at subsites S2 and S3 simultaneously. Smaller and less hydrophobic side chains than typical aromatic rings at residue 169 tended to bipartite substrate binding at subsites S2 and S3, as is seen for W169L, W169V, and W169H. The typical stacked structure of two side chains can not be formed in the former two mutants, which have no planar aromatic rings in the side chains of residues 210 and 169, leading to weaker side chain interaction compared with the His 210–Trp 169 pair. As a result, conformation around residue 169 in W169L/V is likely to be locally disordered and destabilized compared with native API, causing significantly looser substrate binding at subsites S2 and S3 in these non-aromatic mutants. Deviation of these two mutants from a linear relation in the K_m-surface area/hydrophobicity plot may be explained by such a local structural disorder.

In the case of W169H, the formation of aromatic-aromatic stacking is structurally possible between His 210 and His 169. However, Trp and His at residue 169 differ critically in that the indole ring, unionizable in the physiological pH range, is much larger and more hydrophobic than the ionizable imidazole ring. As discussed later, the size and hydrophobicity of the side chain at position 169 are important factors to lower the K_m by shielding the His 210 side chain from the solvent. Since the imidazole ring is hydrophilic, it is likely that His 169 has only a weak shielding effect on His 210 compared with Trp 169. This insufficient shielding of His 210 in W169H may cause significant deviation from the linear relationship in the K_m-surface area plot.

A more detailed consideration of the role of the His 210–Trp 169 interaction is possible based on the three-dimensional structure of API. In this structure, Trp 169 is exposed (accessible surface area, 127 Å^2) and His 210 is buried (28 Å^2). Trp 169 exists far from substrate P1, P2, and P3 residues, and it would be structurally impossible for it to interact directly with atoms of the bound tripeptide substrate. Accordingly, it is only possible that this aromatic residue indirectly exerts its effect on the function of the substrate-binding subsite. In this indirect interaction, His 210 acts as a sole potential mediator for Trp 169 to play its functional role, which is to activate subsites S2 and S3 autonomously to strengthen the substrate binding. For API to efficiently hydrolyze lysyl peptide bonds in a variety of lysine substrates, the stacking of these two aromatic rings is critical and indispensable to potentiate the catalytic power of the active site. The result of the molecular dynamics simulation unraveled that the behavior of this aromatic stacking as a single structural entity supports this idea.

The present investigation provided evidence that the novel His 210–Trp 169 stacking interaction is responsible for enhancing the lysylendopeptidase activity of API. The major role of this aromatic–aromatic interaction is thought to strengthen the binding of substrate at subsite S2 and S3 irrespective of hydrophobicity at subsite P2 and P3. In addition, His 210 is disposed close to the carboxyl group of Asp 113 (3.4 Å for Asp 113 Cγ-His 210 Nδ1), a component of the catalytic triad. It is possible that His 210 sterically compresses the dynamics of Asp 113, as proposed for Asp 102 in salmon trypsin (*22*). If similar steric compression occurs in API, the carboxylate of Asp 113 would be fixed to maintain hydrogen bonding to His 57 in the catalytic triad and increase the population of the functionally "active" conformation of the catalytic triad. This leads the notion that both the catalytic and substrate-binding sites are significantly potentiated by the novel His 210–Trp 169 stacking, which plays an essential role in the generation of the particular catalytic activity of API as a highly active lysylendopeptidase.

We are grateful to Ms. Yoshiko Yagi for the amino acid analysis and Ms. Yumi Yoshimura for the sequence analysis. Thanks are also due to Dr. Ettore Appella for linguistic check of the manuscript.

REFERENCES

1. Stennicke, H.R. and Salvesen, G.S. (2000) Caspase—controlling intracellular signals by protease zymogen activation. *Biochim. Biophys. Acta* **1477**, 299–306
2. Coughlin, S.R. (2000) Thrombin signalling and protease-activated receptors. *Nature* **407**, 258-264
3. Hofmeister, A.E., Londono-Vallejo, A., Harry, E., Stragier, P., and Losick, R. (1995) Extracellular signal protein triggering the proteolytic activation of a developmental transcription factor in *B. subtilis*. *Cell* **83**, 219–226
4. Esmon, C.T. (2000) Regulation of blood coagulation. *Biochim. Biophys. Acta* **1477**, 349–360
5. Brown, M.S. and Goldstein, J.L. (1999) A proteolytic pathway that controls the cholesterol content of membranes, cells, and blood. *Proc. Natl. Acad. Sci. USA* **96**, 11041–11048
6. Boldin, M.P., Goncharov, T.M., Goltsev, Y.V., and Wailach, D. (1996) Involvement of MACH, a novel MORT1/FADD-interact-

ing protease, in Fas/APO-1- and TNF receptor-induced cell death. *Cell* **85**, 803–815
7. Perona, J.J. and Craik, C.S. (1995) Structural basis of substrate specificity in the serine proteases. *Protein Sci.* **4**, 337–360
8. Czapinska, H. and Otlewski, J. (1999) Structural and energetic determinants of the S1-site specificity in serine proteases. *Eur. J. Biochem.* **260**, 571–595
9. Coughlin, S.R. (1999) How the protease thrombin talks to cells. *Proc. Natl. Acad. Sci. USA* **96**, 11023–11027
10. Bode, W. and Huber, R. (2000) Structural basis of the endoproteinase-protein inhibitor interaction. *Biochim. Biophys. Acta* **1477**, 241–252
11. Masaki, T., Nakamura, K., Isono, M., and Soejima, M. (1978) A new proteolytic enzyme from *Achromobacter lyticus* M497-1. *Agric. Biol. Chem.* **42**, 1443–1445
12. Tsunasawa, S., Masaki, T., Hirose, M., Soejima, M., and Sakiyama, F. (1989) The primary structure and structural characteristics of *Achromobacter lyticus* protease I, a lysine-specific serine protease. *J. Biol. Chem.* **264**, 3832–3839
13. Masaki, T., Tanabe, M., Nakamura, K., and Soejima, M. (1981) Studies on a new proteolytic enzyme from *Achromobacter lyticus* M497-1. I. Purification and some enzymatic properties. *Biochim. Biophys. Acta* **660**, 44–50
14. Masaki, T., Fujihashi, T., Nakamura, K., and Soejima, M. (1981) Studies on a new proteolytic enzyme from *Achromobacter lyticus* M497-1. II. Specificity and inhibition studies of Achromobacter. *Biochim. Biophys. Acta* **660**, 51–55
15. Sakiyama, F. and Masaki, T. (1994) Lysyl endopeptidase of *Achromobacter lyticus*. *Methods Enzymol.* **244**, 126–137
16. Masaki, T., Takiya, T., Tsunasawa, S., Kuwahara, S., Sakiyama, F., and Soejima, M. (1994) Hydrolysis of S-2-aminoethylcysteinyl peptide bond by *Achromobacter* protease I. *Biosci. Biotechnol. Biochem.* **58**, 215–216
17. Morihara, K., Ueno, Y., and Sakina, K. (1986) Influence of temperature on the enzymic semisynthesis of human insulin by coupling and transpeptidation methods. *Bioochem. J.* **240**, 803–810
18. Norioka, S., Ohta, S., Ohara, T., Lim, S.-I., and Sakiyama, F. (1994) Identification of three catalytic triad constituents and Asp-225 essential for function of lysine-specific serine protease, *Achromobacter* protease I. *J. Biol. Chem.* **269**, 17025–17029
19. Ohara, T., Makino, K., Shinagawa, H., Nakata, A., Norioka, S., and Sakiyama, F. (1989) Cloning, nucleotide sequence, and expression of *Achromobacter* protease I gene. *J. Biol. Chem.* **264**, 20625–20631
20. Kunkel, T.A. (1985) Rapid and efficient site-specific mutagenesis without phenotypic selection. *Proc. Natl. Acad. Sci. USA* **82**, 488–492
21. Hill, C.R. and Tomalin, G. (1981) The kinetics of hydrolysis of some extended aminoacyl-L-phenylalanine methyl esters by bovine chymotrypsin A. *Biochim. Biophys. Acta* **660**, 65–72
22. Heimstad, E.S., Hansen, L.K., and Smalas, A.O. (1995) Comparative molecular dynamics simulation studies of salmon and bovine trypsins in aqueous solution. *Protein Eng.* **8**, 379–388
23. Miller, S., Janin, J., Lesk, A.M., and Chothia, C. (1987) Interior and surface of monomeric proteins. *J. Mol. Biol.* **196**, 641–656